Cellular Signalling 25 (2013) 2613–2624

Contents lists available at ScienceDirect

Cellular Signalling

journal homepage: www.elsevier.com/locate/cellsig

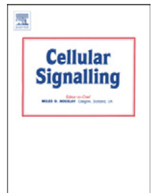

Rapid degeneration of rod photoreceptors expressing self-association-deficient arrestin-1 mutant

Xiufeng Song [a,1,2], Jungwon Seo [a,2,3], Faiza Baameur [a,2], Sergey A. Vishnivetskiy [a], Qiuyan Chen [a], Seunghyi Kook [a], Miyeon Kim [b,4], Evan K. Brooks [b], Christian Altenbach [b], Yuan Hong [a,5], Susan M. Hanson [a,6], Maria C. Palazzo [a], Jeannie Chen [c], Wayne L. Hubbell [b], Eugenia V. Gurevich [a], Vsevolod V. Gurevich [a,*]

[a] Vanderbilt University, Nashville, TN 37232, United States
[b] University of California Los Angeles, Los Angeles, CA 90095, United States
[c] University of Southern California, Los Angeles, CA 90033, United States

ARTICLE INFO

Article history:
Received 7 August 2013
Accepted 23 August 2013
Available online 3 September 2013

Keywords:
Arrestin
Self-association
Monomer
Rhodopsin
Cell death
Retina

ABSTRACT

Arrestin-1 binds light-activated phosphorhodopsin and ensures timely signal shutoff. We show that high transgenic expression of an arrestin-1 mutant with enhanced rhodopsin binding and impaired oligomerization causes apoptotic rod death in mice. Dark rearing does not prevent mutant-induced cell death, ruling out the role of arrestin complexes with light-activated rhodopsin. Similar expression of WT arrestin-1 that robustly oligomerizes, which leads to only modest increase in the monomer concentration, does not affect rod survival. Moreover, WT arrestin-1 co-expressed with the mutant delays retinal degeneration. Thus, arrestin-1 mutant directly affects cell survival via binding partner(s) other than light-activated rhodopsin. Due to impaired self-association of the mutant its high expression dramatically increases the concentration of the monomer. The data suggest that monomeric arrestin-1 is cytotoxic and WT arrestin-1 protects rods by forming mixed oligomers with the mutant and/or competing with it for the binding to non-receptor partners. Thus, arrestin-1 self-association likely serves to keep low concentration of the toxic monomer. The reduction of the concentration of harmful monomer is an earlier unappreciated biological function of protein oligomerization.

© 2013 Elsevier Inc. All rights reserved.

1. Introduction

Rod photoreceptors are highly specialized neurons, where light sensitivity is pushed to the physical limit of single photons [1] at the price of expressing very high concentrations of signaling proteins [2] and consuming enormous amounts of energy [3]. This makes rods very sensitive to a variety of genetic and environmental insults, many of which result in retinal degeneration. Defects in important phototransduction, retinoid cycle, metabolic, or structural proteins cause photoreceptor death [4,5].

Arrestin-1[7] is essential for rapid termination of rhodopsin signaling [6]. Its binding to phosphorylated light-activated rhodopsin (P-Rh*) precludes further transducin activation [7]. Arrestin-1 is expressed in rods [8–11] and cones [12] at a very high level, sufficient to inactivate virtually all photopigment. Arrestin-1 demonstrates exquisite selectivity to phosphorylated light-activated rhodopsin [13,14]. Lack of rhodopsin phosphorylation due to the absence of rhodopsin kinase [15] or mutations eliminating rhodopsin phosphorylation sites [16,17] results in excessive signaling that leads to loss of rod outer segments and rod death. To compensate for phosphorylation defect, we have created transgenic lines expressing arrestin-1-3A (L374A, V375A, F376A) mutant with increased affinity for unphosphorylated light-activated rhodopsin (Rh*) at 50% and 240% of WT level on arrestin-1 knockout (Arr1 −/−) background (3A-50$^{arr1\,-/-}$ and 3A-240$^{arr1\,-/-}$, respectively). We demonstrated normal light sensitivity and recovery kinetics in single cell recordings and electroretinography (ERG) [18], indicating that arrestin-1-3A successfully replaced missing WT arrestin-1. As expected, in the absence of rhodopsin kinase, both 3A-240$^{arr1\,-/-}$ and 3A-50$^{arr1\,-/-}$ lines showed improved

Abbreviations: GPCR, G protein-coupled receptor; GRK, G protein-coupled receptor kinase; WT, wild type; Rh, dark unphosphorylated rhodopsin; Rh*, light-activated unphosphorylated rhodopsin; P-Rh, dark phosphorylated rhodopsin; P-Rh*, light-activated phosphorylated rhodopsin; P-Ops, phospho-opsin.

* Corresponding author at: Department of Pharmacology, Vanderbilt University, Nashville, TN 37232, United States.
E-mail address: vsevolod.gurevich@vanderbilt.edu (V.V. Gurevich).
[1] Present address: Massachusetts General Hospital Cancer Center, GRJ-904, Boston, MA 02114.
[2] These authors equally contributed to this work.
[3] Present address: Wonkwang University, Iksan, Jeollabuk-do, 570–749, South Korea.
[4] Present address: Michigan State University, East Lansing, MI 48824.
[5] Present address: Drexel University, Philadelphia, PA 19104, United States.
[6] Present address: Carroll University, Waukesha, WI 53186, United States.

[7] We use systematic names of arrestin proteins: arrestin-1 (a.k.a. visual or rod arrestin, 48 kDa protein, or S-antigen), arrestin-2 (β-arrestin or β-arrestin1), arrestin-3 (β-arrestin2 or hTHY-ARRX), and arrestin-4 (cone or X-arrestin).

0898-6568/$ – see front matter © 2013 Elsevier Inc. All rights reserved.
http://dx.doi.org/10.1016/j.cellsig.2013.08.022

rod outer segment morphology and functional performance [18]. However, the amplitudes of ERG a- and b-waves were 30–40% lower in 3A-240$^{arr1\ -/-}$ animals than in WT and 3A-50$^{arr1\ -/-}$ line, which parallels the loss of rod photoreceptors seen in 3A-240$^{arr1\ -/-}$ mice [18].

Here we set out to examine the mechanisms of rod degeneration in 3A-240$^{arr1\ -/-}$ mice. We found that rod death induced by high levels of arrestin-1-3A mutant, but not wild type (WT) arrestin-1, was age-dependent but light-independent, ruling out the role of arrestin interactions with light-activated rhodopsin. Historically, arrestin-1 studies focused on its interactions with rhodopsin [19]. However, significant amounts of arrestin-1 are invariably detected in rod synaptic terminals [20–22]. Evidence of rhodopsin-independent arrestin-1 functions are only beginning to emerge [22,23]. In 3A-240$^{arr1\ -/-}$ mice, rod terminals appear to be affected before massive loss of rods, suggesting a role for arrestin-1-3A interaction with non-receptor partner(s) in rod death. Importantly, high expression of WT arrestin-1 is not harmful to rods, and co-expression of WT arrestin-1 partially protects against deleterious effects of the mutant.

2. Materials and methods

2.1. Materials

All restriction and DNA modifying enzymes were from New England Biolabs (Ipswich, MA). All other reagents were from Sigma-Aldrich (St. Louis, MO).

2.2. Transgenic mice expressing WT arrestin-1 and 3A mutant

Animal research was conducted in compliance with the NIH Guide for the Care and Use of Laboratory Animals and approved by the Vanderbilt Institutional Animal Care and Use Committee. WT mouse arrestin-1 and arrestin-1-3A mutant with triple alanine substitution in the C-tail (L374A, V375A, F376A) (that binds Rh* ~10 times better than WT [24]) were transgenically expressed. To this end, the coding sequence with extended 5′- and 3′-UTRs followed by mp1 polyadenylation signal was placed under the control of the pRho4-1 rhodopsin promoter [25] and used to create transgenic mice, as described [9,10,18,19,26,27]. All transgenic lines were bred into Arr1 −/− background [6] to obtain mice where the mutant is the only arrestin present in photoreceptors. The transgene was maintained in hemizygous state by breeding transgenic lines on Arr1 −/− background with transgene-negative Arr1 +/+, Arr1 +/−, and Arr1 −/− mice to obtain necessary control littermates. The expression of transgenic arrestin and rhodopsin was quantified by Western blot in the homogenates of whole eyecups, using the corresponding purified proteins to construct calibration curves [18,26]. Three transgenic lines WT-120, 3A-50, and 3A-240 expressing WT or 3A arrestin-1 at 120%, 50%, and 240% of WT levels, respectively, on Arr1 −/−, Arr1 +/−, and Arr1 +/+ backgrounds were used in this study.

2.3. The analysis of the ONL histology

Mice of either sex were maintained under controlled ambient illumination on a 12 h light/dark cycle. The cages of dark-reared mice were kept in light-proof ventilated boxes from birth, and the husbandry was performed under IR illumination. At indicated ages mice were sacrificed by overdose of isoflurane, the eyes were enucleated and fixed in 4% paraformaldehyde at 4 °C overnight, cryoprotected with 30% sucrose in phosphate-buffered saline, pH 7.2 (PBS) for 6 h, and frozen at −80 °C. Sections (30 μm) were cut on a cryostat and mounted on polylysine (0.1 μg/ml) coated slides. The sections were rehydrated for >40 min in PBS, permeabilized for 10 min in PBS with 0.1% Triton X-100, washed twice for 5 min in PBS, and stained with NeuroTrace 500/525 green fluorescent Nissl (Invitrogen) in PBS (dilution 1:100) for 20 min. The sections were then washed with PBS with 0.1% Triton X-100 for 10 min, and with PBS (2×5 min). Mounted sections were analyzed by confocal microscopy (40× oil objective) (LSM510; Zeiss, Oberkochen, Germany). The outer nuclear layer (ONL) was visualized by fluorescence in FITC (green) channel, outer segments (OS) were viewed with DIC (phase contrast). Two-channel images were acquired for quantitative analysis. Nissl stains nucleic acids, providing a convenient method of prominently labeling DNA-rich nuclei, yielding characteristic diffuse staining of RNA-rich IS (Fig. 1). It also helps to identify nucleic acids-free OS that are clearly visible in DIC image (Fig. 3). The images were collected at the depth where all retinal layers were clearly visualized.

The thickness of ONL was measured on green channel images using IPLab Version 3.9.2 (Scanalytics, Inc.). The retinas of at least three mice (three sections per mouse) for each genotype were used. Each side of the section was divided into three segments according to the distance from optical nerve: central, medium, and peripheral in both inferior and superior hemispheres, so that the whole length of the section was divided into six segments. The measurements were performed at five points spaced at equal distances within each segment using the length measurement tool provided by the software. The images were calibrated using the microscope ruler tool, and all measurements were obtained in μm. Average values of each parameter for individual animals were used to calculate the mean and SD for each genotype.

2.4. The analysis of the OPL histology

The OPL was stained with rabbit anti-NSF antibody (H-300, Santa Cruz Biotechnology). The 30 μm cryosections were blocked free-floating in PBS/0.3% Triton X-100/5% BSA for 1 h at room temperature (RT) and then incubated overnight at 4 °C with primary antibody at 1:500 dilution. After washing in PBS, sections were incubated with mouse biotinylated anti-rabbit antibody (Vector Laboratories, 1:200) for 1 h at RT, washed in PBS, and incubated with streptavidin-Alexa-488 (Invitrogen; 1:200) for 1 h at RT. Some sections were counterstained with fluorescent red Nissl NeuroTrace 530/615 (Invitrogen; dilution 1:200) to label nuclear layers. After extensive washing, sections were mounted on Vectabond-coated slides and cover-slipped with Vectashield (both from Vector Laboratories). Mounted sections were imaged by confocal microscopy (LSM510; Zeiss, Oberkochen, Germany). The green channel images were acquired for quantification; dual channel were used for illustration purposes only.

The thickness of OPL was measured using NIS-Elements-AR software (Nikon). The retinal subdivisions were defined as described above for ONL. The measurements were performed at five points spaced at equal distances within each segment. Average values of each parameter for individual animals were used to calculate the mean and SD for each genotype.

2.5. Detection of apoptotic cells with terminal deoxynucleotidyl transferase (TdT)-mediated dUTP nick end labeling (TUNEL)

In Situ Cell Death Detection kit, Fluorescein (Roche) was used following manufacturer's instructions for the TUNEL staining of 30 μm cryosections. The sections were permeabilized by 0.1% Triton-X100 in 0.1% sodium citrate for 90 min, washed in PBS (5 min + 10 min), mounted on slides, and incubated with TUNEL reaction mixture for 60 min at 37 °C in a humidified atmosphere in the dark. The samples were washed three times with PBS, air-dried, and immersed into mounting medium with DAPI (Vector Laboratories, Inc, CA). Samples were analyzed by fluorescence microscopy. TUNEL-positive cells were detected in FITC (green) channel. Photoreceptor death rate was estimated as the proportion of TUNEL positive cells in the ONL (the number of TUNEL-positive cells divided by the total number of DAPI-stained nuclei). TUNEL-positive cells were counted on the whole length of each section; four sections were examined for each age and genotype to calculate means and SD.

Download English Version:

https://daneshyari.com/en/article/10816139

Download Persian Version:

https://daneshyari.com/article/10816139

Daneshyari.com